Scale-Dependent Effects of Bank Vegetation on Channel Processes: Field Data, Computational Fluid Dynamics Modeling, and Restoration Design

Brian P. Bledsoe,[1] Shaun K. Carney,[1,2] and Russell J. Anderson[1,3]

Bank vegetation substantially influences flow resistance, velocity, shear stress distributions, and geomorphic stability in many natural river settings. We analyze field data from gravel bed streams with typed bank vegetation characteristics and employ three-dimensional computational fluid dynamics (CFD) modeling to examine whether the effects of bank vegetation on channel form and processes are scale dependent. Field data from the United States and United Kingdom indicate that mean bankfull dimensionless shear stresses are significantly higher in channels with thick woody vegetation but only for channel widths less than ~20 m. Because specific mechanisms controlling the apparent scale dependency are difficult to isolate in natural channels, we develop CFD models of streams with coarse beds and bank vegetation to investigate physical processes in channels with variable bed and bank roughness. The CFD models are applied in two sets of simulations to improve mechanistic understanding of patterns in the field data and to examine (1) spatial scale dependency between channel width and vegetation effects and (2) the coevolution of flow hydraulics, channel form, and vegetation establishment. The scale-dependent bank vegetation effects on shear stress distributions in the CFD representations are consistent with field data from gravel bed streams and suggest that the length scale of bank vegetation protrusion relative to channel width is an important factor that could improve shear stress partitioning models. In general, the field data and CFD simulations indicate a significant scale-dependent effect of bank vegetation with important implications for stream restoration designs based on tractive force, regime, and analytical approaches.

1. INTRODUCTION

Bank vegetation along streams and rivers performs important ecological and geomorphic functions by influencing flow hydraulics, channel form and stability, and habitat diversity. Stream restoration plans frequently include reestablishment of bank vegetation to increase geotechnical stability of banks due to root reinforcement [*Abernethy and Rutherfurd*, 2000; *Simon and Collison*, 2002], influence flow patterns in streams and decrease near-bank velocities [*Thorne and Furbish*, 1995]. Decreased flow velocities in the vicinity of vegetated banks can significantly alter distributions of shear stress and sediment transport across the entire channel

[1]Department of Civil and Environmental Engineering, Colorado State University, Fort Collins, Colorado, USA.
[2]Now at Riverside Technology, Inc., Fort Collins, Colorado, USA.
[3]Now at Morrison-Maierle, Inc., Helena, Montana, USA.

Stream Restoration in Dynamic Fluvial Systems: Scientific Approaches, Analyses, and Tools
Geophysical Monograph Series 194

10.1029/2010GM000959

and particularly in the near-bank region. Many researchers have found riparian vegetation significantly influences channel form, including hydraulic geometry [*Charlton et al.*, 1978; *Andrews*, 1984; *Hey and Thorne*, 1986; *Soar and Thorne*, 2001], planform characteristics [*Millar*, 2000], and scour pool characteristics [*Gran and Paola*, 2001]. Bank and floodplain vegetation also affect stage-discharge relationships in rivers, and specific methods for estimating flow resistance due to riparian vegetation have been previously developed [*Darby and Thorne*, 1996; *Darby*, 1999].

Previous work on the influence of bank vegetation on flow hydraulics has typically focused on empirically estimating increases in channel resistance due to vegetation [*Coon*, 1998], partitioning resistance between vegetated and nonvegetated portions of the channel [*Darby and Thorne*, 1996; *Darby*, 1999; *Yen*, 2002], or computing average flow profiles over or through vegetation [*Fischenich*, 1996]. *Fischenich* [1997] and *Lopez and Garcia* [1997] provide reviews of many of the basic qualitative and quantitative methods of accounting for channel vegetation.

Previous research also suggests that the influence of bank vegetation is scale dependent [*Anderson et al.*, 2004]. For example, *Coon* [1998] investigated the influence of bank vegetation on Manning's roughness coefficient and concluded that the influence was minimal in channels wider than about 20 m and could not be discerned in channels wider than approximately 30 m. Likewise, modeling by *Masterman and Thorne* [1992] indicates that the effects of riparian vegetation on flow hydraulics is limited when width-to-depth ratios increase beyond about 15. A better understanding of the fundamental processes controlling channel form and stability in terms of scale-dependent influence of vegetation on flow hydraulics would benefit channel evolution modeling, characterization of material fluxes and instream habitats, and stream restoration design.

Although field investigations could further clarify these processes, field measurements of detailed flow fields in the vicinity of vegetation are difficult to collect due to the infrequency of high-flow events that inundate vegetated banks and the associated measurement difficulties during high flows. Furthermore, finding multiple stream reaches with similar characteristics is challenging due to differences in vegetation characteristics, nonvegetative form roughness, sediment supply, flow regime, anthropogenic disturbance, and other influences. Physical modeling provides another tool for analyzing the influence of vegetation, but can be costly and time consuming. Selecting appropriate variable test ranges and scaling factors for vegetation and channel dimensions can also be challenging. Numerical modeling is an attractive alternative, provided that vegetation can be appropriately represented.

Computational fluid dynamic (CFD) modeling offers an increasingly viable means of analyzing the influence of bank vegetation on channel hydraulics and form in a variety of applications. With a growing number of CFD software packages and advances in computational efficiency, two-dimensional (2-D) and three-dimensional (3-D) modeling of river flow problems have become more feasible and widely utilized. CFD has been utilized to investigate many complex flow situations typical to natural channels [e.g., *Bradbrook et al.*, 1998; *Nicholas and Sambrook-Smith*, 1999; *Booker et al.*, 2001; *Morvan et al.*, 2002; *Rameshwaran and Naden*, 2003; *Nicholas and McLelland*, 2004], model erosion and sedimentation patterns [e.g., *Wu et al.*, 2000; *Shams et al.*, 2002], and study habitat suitability for fish species [e.g., *Crowder and Diplas*, 2000; *Booker*, 2003]. In CFD modeling, detailed 3-D velocity fields and shear stress distributions can be resolved for a given channel geometry. CFD modeling also offers the advantage of allowing the investigation of a variety of cases and scenarios with less labor and expenses than would be required to complete comparable physical experiments and can be used to design and optimize physical modeling efforts. The commercially available CFD package FLUENT [*Fluent Inc.*, 2003] has been widely applied to model open-channel flows [e.g., *Nicholas and Sambrook-Smith*, 1999; *Nicholas*, 2001; *Gessler and Meroney*, 2002; *Ma et al.*, 2002; *Shams et al.*, 2002; *Prinos et al.*, 2003; *Nicholas and McLelland*, 2004].

In this study, we (1) analyze field data from gravel bed streams and rivers in the United States and United Kingdom with various bank vegetation characteristics and (2) employ 3-D CFD modeling in FLUENT to examine the influence of bank vegetation in gravel bed channels and whether the effects of bank vegetation on key hydraulic parameters used in restoration design of gravel bed streams are scale dependent. We hypothesize that in relatively narrow channels, dense woody vegetation protruding appreciably into the bankfull flow field results in significantly higher values of bankfull dimensionless shear stress (τ_*) and slope (S). In the CFD modeling experiments, a drag force representation of vegetation [e.g., *Fischer-Antze et al.*, 2001] is coupled with the porous treatment of bed roughness described by *Carney et al.* [2006] to investigate the influence of bank vegetation on flow hydraulics in trapezoidal channels. The resulting model is used to elucidate processes responsible for patterns observed in the field data and to specifically examine (1) scale dependency of vegetation influence in channels with similar characteristics but different widths and (2) changes in flow hydraulics following a succession of vegetation establishment along a channel. CFD modeling results are compared with data from natural channels of various scales with typed bank vegetation to examine the magnitude and scale

dependency of hydraulic effects. Finally, implications for geomorphic analysis, CFD modeling, and restoration design of natural gravel channels with successional bank vegetation are discussed.

2. METHODS

2.1. Analysis of Field Data

We compared mean values of bankfull dimensionless shear stress (τ_*) for channels with different bank vegetation conditions using data from field studies of gravel bed streams and rivers in the western United States by *Andrews* [1984] and in the United Kingdom by *Charlton et al.* [1978] and *Hey and Thorne* [1986]. These studies were selected because bank vegetation was typed for each study site, and the data sets contain the necessary geomorphic and hydraulic data for examining τ_* as it varies with channel width and vegetation type. Bankfull dimensionless shear stress is referenced to the median grain size (D_{50}) and defined as

$$\tau_* = \frac{RS}{(G-1)D_{50}}, \quad (1)$$

where R is hydraulic radius, S is slope, and G is the specific gravity of sediment assumed to equal 2.65.

Throughout this chapter, bank vegetation conditions are referred to as "thick" or "thin." If percent coverage data were available, "thick" vegetation refers to bank vegetation qualitatively described by the researchers as forested, heavy, or thick vegetated bank conditions with greater than 5% tree/shrub cover. "Thin" vegetation refers to grass-covered banks, nonforested channels, or channels where tree/shrub coverage is less than 5%. It should be noted that thick does not equate to density, as grasses may be much denser than woody vegetation on a stem per area basis. Thus, the term thick is best described as a qualitative index of woody vegetation dominance (density, basal area, and coverage) that is directly related to the stiffness and length scale of bank roughness elements [*Anderson et al.*, 2004].

Mean comparisons of τ_*, relative submergence (R/D_{90}, R/D_{84}, and h/D_{84} for the *Andrews* [1984], *Charlton et al.* [1978], and *Hey and Thorne* [1986] data sets, respectively), substrate gradation D_{84}/D_{50} (D_{90}/D_{50} for *Andrews* [1984]), and S between channels of differing sizes and bank vegetation types were performed using Student's t tests [*Snedecor and Cochran*, 1989]. Following *Coon* [1998], channels with top widths <20 m were considered as one group and those ≥20 m as another. In each group, mean values of dimensionless shear stress were compared between channels with thick versus thin bank vegetation. In all cases, a test for equal variance was conducted using an F test, and a modified t test was performed when the variances were not equal. We used one-tailed tests for τ_* and S of channels <20 m wide, and two-tailed tests for all others.

To test for scale-dependent effects of thick bank vegetation on stable channel slope, we developed multivariate power function models of the form $S = f(Q, D_{84})$ where Q is discharge ($m^3\ s^{-1}$), and D_{84} is the 84th percentile of grain size (m) for the *Hey and Thorne* [1986] and *Charlton et al.* [1978] data sets using standard multiple regression techniques. Models were fit with and without a "toggle" variable that shifted the model intercept for observations with both thick vegetation and a top width <20 m to test for a significant scale-dependent effect of vegetation. Sediment transport capacity was not included as a predictor variable as in the *Hey and Thorne* [1986] analysis because it could potentially confound the results due to a lack of shear stress partitioning that accounts for vegetation influences. The *Andrews* [1984] data were not included in the regressions because D_{84} values were not reported.

2.2. CFD Simulations of Bank Vegetation Influence

Two types of CFD modeling simulations were performed to examine some of the fundamental vegetative controls on channel hydraulics and to demonstrate the utility of the modeling approach developed in this study. The first set of simulations addresses the spatial scale dependence of the influence of bank vegetation in channels of varying width. The second set of simulations examines the evolving hydraulics of vegetated streams due to either natural regeneration of vegetation following a disturbance event (e.g., postflood) or accelerated vegetation establishment following rehabilitation or restoration activities.

Previous studies have not included a channel width versus lateral vegetation roughness length scale term to quantify potential scale-dependent effects on hydraulic behavior. The first set of simulations focused on our hypothesis that width relative to lateral protrusion of bank vegetation could be an important factor in channels <20 m wide. In these simulations, channel bank angle, slope, depth, grain-size distribution, and vegetation characteristics (shape extending into the channel and inertial loss coefficient) were all held constant for each run. The porous zone representing vegetation was given a $C_D A_v$ value of 11.5 m^{-1} reported for natural channels by *Fischenich* [1996], where C_D is a drag coefficient, and A_v is a measure of vegetation density (L^{-1}). Using a periodic boundary condition, the discharge was adjusted to maintain a constant depth of flow, and channel slope was held constant for each run. The width of the channel was then varied between each configuration to simulate different channel

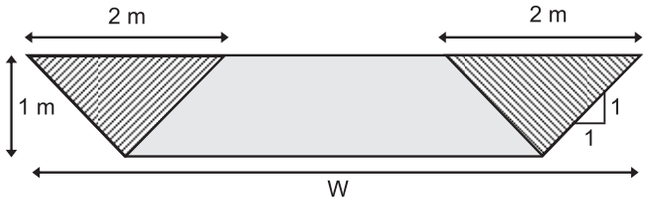

Figure 1. Channel configurations for the scale-dependent simulations. Width is the only channel characteristic changing among simulations (S_o = 0.001; D_{84} = 50 mm; $C_D A_v$ = 11.5 m^{-1} for the vegetation on both banks). The hashed region on both banks represents the shape of the vegetation zone extending into the channel. The depth and slope were held constant, and discharge was varied.

sizes (Figure 1). For each configuration, one realization was performed with bank vegetation, and another was made without bank vegetation.

Following disturbances such as large floods, fires, grazing, or clearing, vegetation will often regenerate in stream riparian areas. Reestablishing vegetation on stream banks is also a common strategy of stream restoration. Whether natural regeneration or accelerated reestablishment due to rehabilitation efforts, bank vegetation typically is sparse immediately following disturbance or implementation of a restoration plan. Thus, the influence of bank vegetation on flow hydraulics evolves as density, stiffness, and protrusion change over time.

In the second set of model simulations, we simulated vegetative succession in a channel of fixed characteristics (width, side slope, bed roughness, and channel slope) with four vegetation treatments. In the first case, no vegetation was simulated, and channel roughness was limited to the porous treatment of the bed. In each subsequent scenario, simulated vegetation is included on the banks of the channel with incrementally greater amounts of protrusion. The protrusion of the simulated vegetation into the channel is increased in each scenario by lowering the minimum elevation of vegetation on the bank. The inertial loss coefficient of the vegetation zones is increased to simulate increasing flow resistance as vegetation matures and becomes denser and stiffer. Channel slope was set through the pressure gradient in the periodic boundary condition. Flow depth was then varied by iteratively regridding the domain and rerunning the solver until an equal discharge (±1%) was achieved for all scenarios.

2.3. Background on CFD Modeling Approach

Numerous researchers have recognized the potential CFD modeling provides for geomorphic analyses involving vegetation. In CFD, roughness is typically parameterized using a roughness length in some form of logarithmic velocity equation [e.g., *Hey*, 1979]. The representation of boundary roughness using a roughness length inadequately represents the physical processes creating flow profiles over and through vegetation. Alternative modeling methods have been proposed based on drag force representations of vegetation. *Shimizu and Tsujimoto* [1994] proposed the addition of a sink term in the governing momentum equations based on the drag due to vegetation. The drag force was parameterized as a function of vegetation density and drag coefficients. In the *Shimizu and Tsujimoto* [1994] model, two additional terms are included in the turbulent kinetic energy and turbulence dissipation rate equations of the k-ε turbulence model to account for the additional effects of vegetation on turbulence. These terms were also a function of the vegetation density and drag coefficients, but were treated as calibration parameters. Detailed flow observations through vertical rods in a laboratory flume were used to calibrate and verify their model.

Lopez and Garcia [1997] developed a similar vegetation representation based on atmospheric science studies [*Raupach and Shaw*, 1982]. Their model also used vegetation density and associated drag coefficients to represent vegetation, although they gave a theoretical basis for two additional terms included in the turbulent kinetic energy and turbulence dissipation rate equations. Their model was also compared to detailed velocity measurements in a flume setting, with vegetation represented as either stiff or flexible submerged dowels.

Fischer-Antze et al. [2001] noted differences among model coefficients used in the *Shimizu and Tsujimoto* [1994] and *Lopez and Garcia* [1997] studies, and postulated that the turbulent diffusive terms introduced by both modelers were of minor importance relative to the drag term in the momentum equations. In the *Fischer-Antze et al.* [2001] model, the same vegetation representation is utilized to include a drag force in the momentum equations without modifications to the turbulence equations of the k-ε model. Using the same data sets as *Shimizu and Tsujimoto* [1994] and *Lopez and Garcia* [1997], *Fischer-Antze et al.* [2001] added a third flume data set [*Pasche*, 1984] and demonstrated that velocity profiles of similar accuracy could be captured without turbulence model modifications. We also use these data sets to verify model simulations as described below.

Each of the above studies presented different vegetation modeling methods and compared the results with laboratory flume data, but did not extend those studies to natural channels or use the models to investigate the geomorphic influence of vegetation in open-channel flow. *Kean and Smith* [2004] present a simplified model based on an algebraic turbulence closure with vegetation represented using similar

drag force concepts. After developing their model and presenting a verification based on the *Pasche* [1984] flume data set, *Kean and Smith* [2004] use the model to investigate the impacts of vegetation on shear stress distributions in straight, clay-bed, prismatic channels. Although the model may be simpler to implement, its applicability is limited to relatively simple channel geometries. In a different application, *Nicholas and McLelland* [2004] used CFD to model overbank flow through vegetation by implementing the *Fischer-Antze et al.* [2001] representation of vegetation, a roughness length representation of boundary roughness, and a renormalized group theory (RNG) k-ε turbulence closure model. *Nicholas and McLelland* [2004] recognized the potential to utilize a simple drag force representation of vegetation to reproduce velocity and turbulence profiles in the vicinity of vegetation, yet they noted the inherent challenges associated with determining appropriate model parameters to represent vegetation.

In the present study, the vegetation representation of *Fischer-Antze et al.* [2001] is implemented. Vegetative resistance is parameterized in terms of a drag coefficient and a measure of vegetation density:

$$\frac{F_{D,i}}{V_{\text{fluid}}} = \frac{1}{2}\rho C_D A_v u_{\text{mag}} u_i, \tag{2}$$

where $F_{D,i}$ is the drag force in the ith (x, y, or z) direction, V_{fluid} is the fluid volume over which the drag force is applied (equal to unity), ρ is density of the fluid-sediment mixture (assumed equal to 1000 kg m^{-3}), u_{mag} is the resultant reference velocity magnitude, and u_i is the reference velocity in the ith direction (the velocity which would be present if the stem being acted upon were removed from the flow [*Kean and Smith*, 2004]). If the resistance due to vegetation is due primarily to rigid stems that can be modeled as rigid cylinders, the value of A_v may be determined from:

$$A_v = nD_s = \frac{D_s}{\lambda^2}, \tag{3}$$

where n is number of stems per unit area, D_s is average stem diameter, and λ is average stem spacing (L). *Shimizu and Tsujimoto* [1994], *Lopez and Garcia* [1997], *Fischer-Antze et al.* [2001], and *Kean and Smith* [2004] all represent vegetative resistance in the form presented in equations (2) and (3). Alternatively, *Fischenich* [1996] and *Fischenich and Dudley* [2000] compiled numerous data sets (primarily *Rahmeyer et al.* [1995]) and presented methods for computing $C_D A_v$ for different riparian vegetation species. Their data sets are based on flume studies involving actual vegetation species assemblages. These sources provide an alternative means of estimating drag coefficients and representative areas for typical riparian vegetation without representing vegetation as a field of rigid cylinders. The range of representative $C_D A_v$ values used in the present study was extracted from *Fischenich* [1996].

The vegetative resistance computed according to equation (2) is included as a source term in the governing momentum equations. Assuming the turbulent diffusive terms due to vegetation are dominated by the vegetative drag term per *Fischer-Antze et al.* [2001], the drag force may be applied through the use of a porous media zone in FLUENT without modification to the turbulence models. *Carney* [2004] demonstrated that the vegetation representation used in this study could be coupled with the RNG k-ε turbulence model to reasonably reproduce the laboratory velocity profiles of *Tsujimoto et al.* [1991], *Dunn et al.* [1996], and *Pasche* [1984]. *Carney* [2004] also conducted grid-dependency tests to quantify the uncertainty in simulated results following *Hardy et al.* [2003] for the flume study verification model runs. The mean absolute percentage error in simulated downstream velocities among different resolution grids was less than 5% for all tested cases. The grids used for the case studies were of a similar resolution to those generated for the grid-dependency tests and contained 25 to 30 vertical cells with similar resolution horizontally. Cells were more closely concentrated in regions where higher velocity gradients were expected. A typical grid used in this simulation is shown in Figure 2.

2.3.1. Bed roughness representation. CFD modeling of coarse-grained channels can be challenging due to difficulties with roughness parameterization [*Nicholas*, 2001] as the maximum roughness length is limited to half the thickness of the near-bed cells [*Fluent Inc.*, 2003]. *Carney et al.* [2006] adapted the model of *Wiberg and Smith* [1991] to represent coarse-bedded channels in CFD. In this approach, the drag force per unit volume acting over the height of the D_{84} grain size is:

$$\frac{F_{D,\text{total}}(z)}{V_{\text{total}}} = c_b \frac{\frac{\rho}{2} C_D \frac{\pi}{4} D_{\text{my}} D_{\text{mz}} u(z)^2}{\frac{\pi}{6} D_{\text{mx}} D_{\text{my}} D_{\text{mz}}} = \frac{3}{4}\rho \frac{c_b C_D}{D_{84x}} u(z)^2, \tag{4}$$

where c_b represents the inverse of the average porosity of the bed, D_{mx}, D_{my}, and D_{mz} are the grain dimensions in

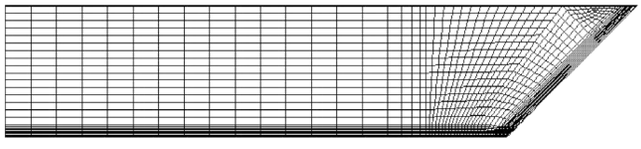

Figure 2. Computational grid (cross-section view, half channel) for the second set of simulations.

the downstream, cross-sectional, and vertical directions, respectively, and the drag force at a level z between the top and bottom of a grain, $F_D(z)$, is computed by replacing the average velocity with the velocity at the height z, $u(z)$. A zone is created adjacent to the bed the height of the D_{84} grain size, and a momentum sink term defined according to equation (2) is assigned to this zone. In the FLUENT application, the above may be accomplished using a porous media zone [*Carney et al.*, 2006]. Field observations indicate that c_b typically takes a value of about 0.6, which is used in this model [*Wiberg and Smith*, 1991]. The value of C_D is set to 0.45 based on drag relationships for spheres [*Coleman*, 1967].

Shear stress at a channel boundary is typically computed in CFD using a wall function. However, when bed roughness is represented using the above approach, the channel wall is located below the grains composing the bed. Therefore, shear stresses were computed at the top of the D_{84} particle size for comparisons among model runs based on the Reynolds stress and molecular shear stress at a point:

$$\tau_{ij} = (\mu + \mu_e)\left(\frac{\partial u_i}{\partial x_j} + \frac{\partial u_j}{\partial x_i}\right), \tag{5}$$

where μ is the molecular viscosity, μ_e is the eddy viscosity (computed by the turbulence model), and u_i and u_j are the velocities in the x_i and x_j directions, respectively. The resultant of the applied forces was taken to determine the total shear stress at a point. The average bed shear ($\tau_{bed,avg}$) could then be computed over the bed of the cross-section according to:

$$\tau_{bed,avg} = \frac{\sum(\tau_{ij} d)_w}{W}, \tag{6}$$

where d is the width of a cell in the cross-stream direction over which the shear stress τ_{ij} is computed, the summation is computed over all cells across the cross-section, and W is the bottom width of the channel. These estimates of average bed shear stress are contrasted with cross-section averaged shear stresses (τ_o) defined as $\tau_o = \rho g R S$.

2.3.2. Additional modeling details. We used the RNG k-ε turbulence model with standard equilibrium wall functions [*Yakhot and Orszag*, 1986]. The RNG k-ε turbulence model has been shown to perform better than the standard k-ε model in natural streams involving complex flow geometry [e.g., *Bradbrook et al.*, 1998] and was utilized by *Nicholas and McLelland* [2004] to model flow through natural vegetation using the same vegetation treatment.

FLUENT discretizes the governing conservation of mass and momentum equations using a finite volume approach [*Fluent Inc.*, 2003]. The momentum equations and turbulence equations were discretized using second-order upwind differencing. SIMPLEC pressure-velocity coupling was utilized, which permitted higher under-relaxation factors (0.8–1.0). The water surface was modeled using a fixed lid approach where the free surface was simulated as a symmetry plane with normal velocity components and normal gradients of all variables equal to zero.

The banks of natural channels exhibit substantial variability as channel meandering characteristics, bed topography such as pool-riffle sequences, or other channel variability influences shear stress, turbulence, and velocity characteristics [*Buffington and Montgomery*, 1999; *Wohl*, 2000; *Nicholas and McLelland*, 2004]. In this study, the objective was to specifically isolate the impact of vegetation on flow hydraulics, and only straight prismatic channels were modeled.

Vegetation characteristics (density, species, maturity, and extent of protrusion into the channel) can vary significantly in a given channel reach and contributes to flow complexity. However, *Carney* [2004] demonstrated that by representing the vegetation in the model with a constant width and density (drag characteristics), the essential flow characteristics could be captured, providing a substantial simplification for modeling.

Modeling prismatic channels with constant vegetation characteristics permitted analysis with a periodic inlet/outlet boundary condition to achieve a fully developed flow profile through the flow domain. With the periodic boundary condition, discharge Q through the domain was adjusted until the slope computed based on the downstream pressure gradient $S_{o,P}$, matches the desired channel slope [*Nicholas*, 2001], where

$$S_{o,P} = \frac{1}{\rho g}\frac{dP}{dx} \tag{7}$$

and g, P, and x are gravitational acceleration, pressure, and downstream distance, respectively. The periodic boundary condition also permits modeling a short reach, reducing computational costs.

3. RESULTS

3.1. Analysis of Field Data Results

Analysis of the three field data sets indicates vegetative effects on shear stress magnitudes and scale dependency in dimensionless shear stress values. Mean values of bankfull dimensionless shear stresses in channels <20 m wide are contrasted with values from wider channels in Table 1. For narrower streams with width <20 m, channels with thick

Table 1. Mean Values of Bankfull Dimensionless Shear Stress (τ_*) Stratified by Bank Vegetation and Channel Size[a]

	Channels With Width <20 m			Channels With Width >20 m		
	Thin	Thick	p Value	Thin	Thick	p Value[b]
Andrews [1984]	0.034	0.058	0.0003	0.038	0.030	0.310
Charlton et al. [1978]	0.032	0.073	0.0040	0.038	0.047	0.397
Hey and Thorne [1986][c]	0.045	0.094	0.0002	0.048	0.050	0.849

[a]Differences in τ_* by vegetation type are significant only for channels <20 m wide.

[b]The p value equals the probability that τ_* for thin vegetation is less than τ_* for thick vegetation in channels <20 m and the probability that τ_* for thin vegetation is different than τ_* for thick vegetation in channel widths >20 m.

[c]Thin indicates Hey and Thorne types 1 and 2; thick indicates Hey and Thorne types 3 and 4.

bank vegetation exhibit significantly higher dimensionless shear stresses than those with thin bank vegetation in each of the data sets investigated. Although the bankfull dimensionless shear stresses in channels with thick vegetation are significantly higher in all three studies ($p < 0.003$), there is no significant difference between dimensionless shear stresses for channels with thick or thin bank vegetation at channel widths >20 m (Figure 3).

Relative submergence in channels with widths <20 m was significantly greater ($p = 0.091$) for channels with thick compared to thin vegetation in the *Hey and Thorne* [1986] data. In all three data sets, slopes of channels <20 m wide with thick vegetation were significantly greater than those of channels <20 m wide with thin vegetation ($p \leq 0.053$). All other t tests were nonsignificant. Multiple regression modeling results were very consistent for the *Charlton et al.* [1978] and *Hey and Thorne* [1986] data sets. The toggle variable representing an effect of thick vegetation on channel slope solely for channels <20 m wide was highly significant for the individual data sets ($p < 0.0012$) and both data sets combined ($p < 0.00002$). Models including the toggle variable for small channels with thick vegetation explained 10% to 15% more variance in slope than models with only Q and D_{84}. The slopes of channels <20 m wide with thick vegetation were on

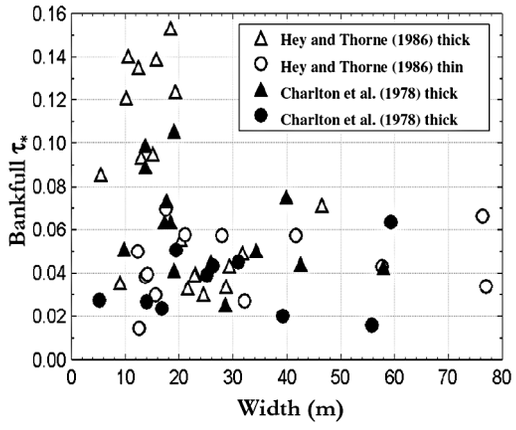

Figure 3. Bankfull dimensionless shear stress referenced to D_{50} for channels with thick and thin bank vegetation. Data are from *Hey and Thorne* [1986] and *Charlton et al.* [1978].

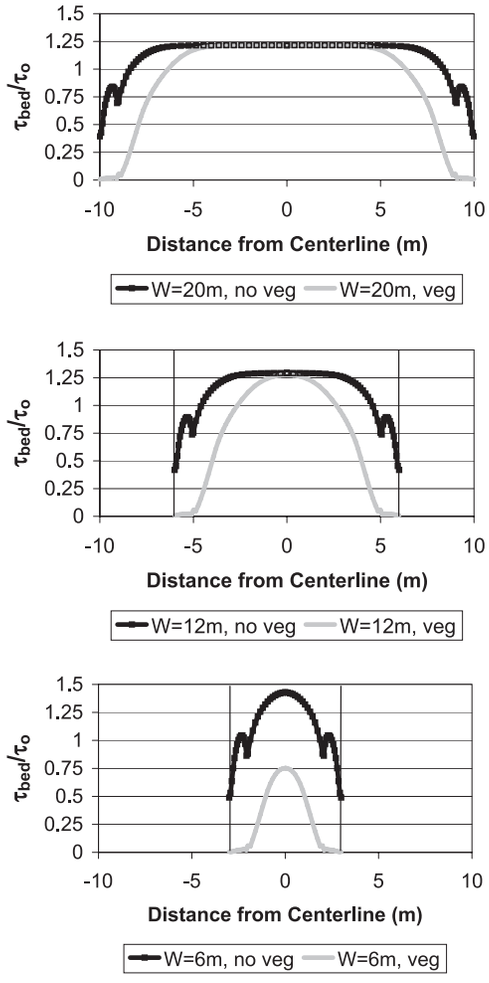

Figure 4. Cross-section boundary shear stress distributions for channels of different widths.

Table 2. Comparison of $\tau_{bed,avg}/\tau_o$ and the Portion of Shear Stress Consumed by the Vegetation for Channels of Different Widths[a]

Top Width (m)	Bed Shear Stress Fraction	Vegetation Shear Stress Fraction
	$\tau_{bed,avg}/\tau_o$	$1 - \tau_{bed,avg}/\tau_o$
6	0.37	0.63
12	0.74	0.26
20	0.86	0.14
30	0.91	0.09

[a]In this case, for consistency of comparison between computed shear stresses, τ_o is computed as the average shear stress over the entire boundary in an unvegetated channel according to equations (5) and (6).

average 60% and 105% steeper for a given combination of Q and D_{84} in the *Hey and Thorne* [1986] and *Charlton et al.* [1978] data sets, respectively.

3.2. Modeling Study Results

3.2.1. Scale-dependent influence of vegetation. For the first modeling scenario, Figure 4 depicts the resulting shear stress distributions along the bed of the channel for selected channel widths. For each channel width, τ_o is equal for the vegetated and unvegetated cases because hydraulic radius and channel slope were held constant for each realization. For a given width, the actual shear stress on the bed of the vegetated channel ($\tau_{bed,avg}$) is less than the shear stress on the bed of the unvegetated channel and reflects the additional energy attenuated by the vegetation. Thus, although τ_o is the same for vegetated and unvegetated channels, shear stress distributions on channel beds differ markedly and depend on channel width.

The largest channel shown in Figure 4 is 20 m wide. The drop in shear stress at the bank toe for the unvegetated channels is due to the trapezoidal channel shape. Comparing the shear stress along the channel bed in vegetated and unvegetated channel scenarios, vegetation affects bed shear stress approximately 6 m into the channel from each bank or approximately 60% of the total width. In the channel center beyond the zone of vegetation influence, shear stresses are virtually identical, regardless of vegetation conditions. For channels wider than 20 m, the same pattern is observed. Simulated vegetation affects the shear stress across the entire perimeter of a 12 m channel (Figure 4), with a much smaller zone in the channel center that remains unaffected by the simulated vegetation. Finally, in channels narrower than about 12 m, a considerable drop in shear stress on the bed of the channel is present under the vegetated case. The ratio of average boundary shear stress to cross-section averaged shear stress for the vegetated channels of different widths are presented in Table 2. In this table, the average shear stress over the bed of the channel is computed using equations (5) and (6). To provide a consistent comparison between the shear stress computed using this method and the cross-section averaged shear stress, the shear stress over the entire boundary in an unvegetated channel is computed using equations (5) and (6). If no other factors contribute to the shear stress, this can be assumed equivalent to τ_o. The vegetation fraction of the total shear stress is over four times greater with the decrement of channel width from 20 to 6 m.

3.2.2. Vegetation reestablishment following disturbance or restoration. For the second set of model simulations focusing on bank vegetation succession, channel characteristics and resulting flow depths with average velocities for each scenario are presented in Table 3. In these scenarios,

Table 3. Channel Characteristics for Scenarios Simulating Establishment of Bank Vegetation[a]

	Scenario			
	1 (No Vegetation)	2	3	4 (Full Vegetation)
Distance from bed vegetation begins (m)	–	0.75	0.5	0.25
$C_D A_v$ (m^{-1})	–	0.4	0.8	1.2
Depth, z above the D_{84} grain height (m)	1	1.01	1.06	1.17
$\bar{u}$ (m s^{-1})	1.28	1.27	1.20	1.07
u_{max} (m s^{-1})	1.80	1.81	1.87	1.95
τ_o(Pa)	24.4	24.5	25.6	27.8
$\tau_{bed,avg}$ (Pa)	25.6	25.6	25.3	23.7
$\tau_{bed,max}$ (Pa)	28.5	28.7	29.9	31.4

[a]Bottom width is 4 m; side slopes equal 1:1; $S_o = 0.003$; $D_{84} = 50$ mm; $Q = 5.75$ m^3 s^{-1}. Depth is measured from the top of the D_{84} grains. Here $\bar{u}$ and u_{max} are the average and maximum downstream velocities for the cross-section, respectively; $\tau_{bed,avg}$ and $\tau_{bed,max}$ are the average and maximum bed shear stress, respectively, computed using equations (5) and (6) at the D_{84} grain height across the channel boundary.

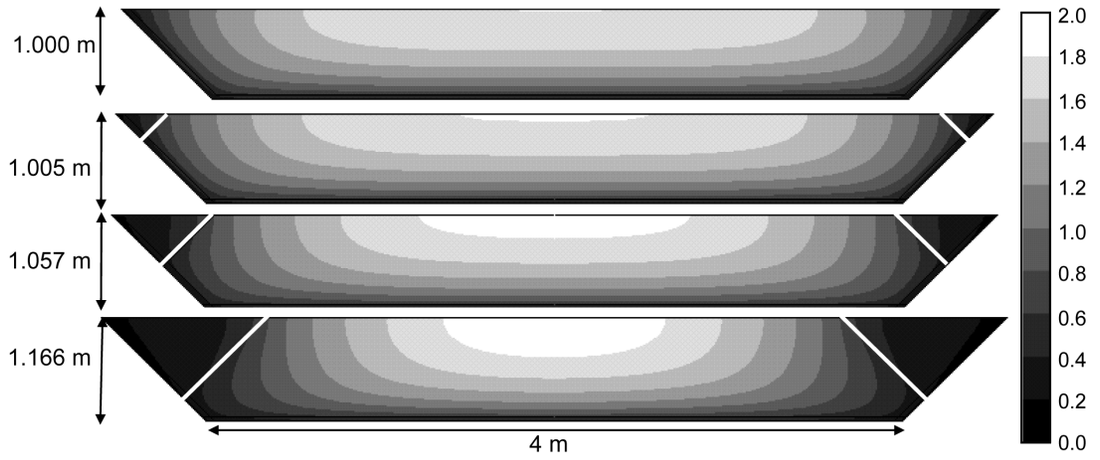

Figure 5. Velocity contours (m s^{-1}) for four increments of simulated vegetation establishment. The white line indicates the edge of the simulated vegetation.

increases in width and depth were necessary to convey a constant discharge. Figures 5 and 6 depict velocity contours and contours of the fluid shear stress computed according to equation (8), respectively, for each of the four scenarios. These simulations indicate that as vegetation establishes on channel banks, near-bank velocities are reduced. Lower velocities in near-bank regions result in an increase in the depth required to convey a constant flow. Accordingly, from the unvegetated scenario (scenario 1) to the scenario with fully established vegetation (scenario 4), there is a 17% increase in the flow depth and a 16% reduction in average velocity. Bank vegetation concentrates flow away from the bank toe and into the channel center. Although there is a large reduction in near-bank velocities due to the vegetation, maximum velocity in the channel center increases 8% from scenarios 1 to 4.

Examination of shear stresses reveals similar patterns (Table 3 and Figure 7). Cross-section averaged shear stress, which was not held constant in these scenarios, increases 14% from scenario 1 to scenario 4 due to increases in flow depth. Average bed shear stress ($\tau_{bed,avg}$) computed according to equations (5) and (6), however, follows an opposite trend and decreases 7% from scenario 1 to scenario 4. The

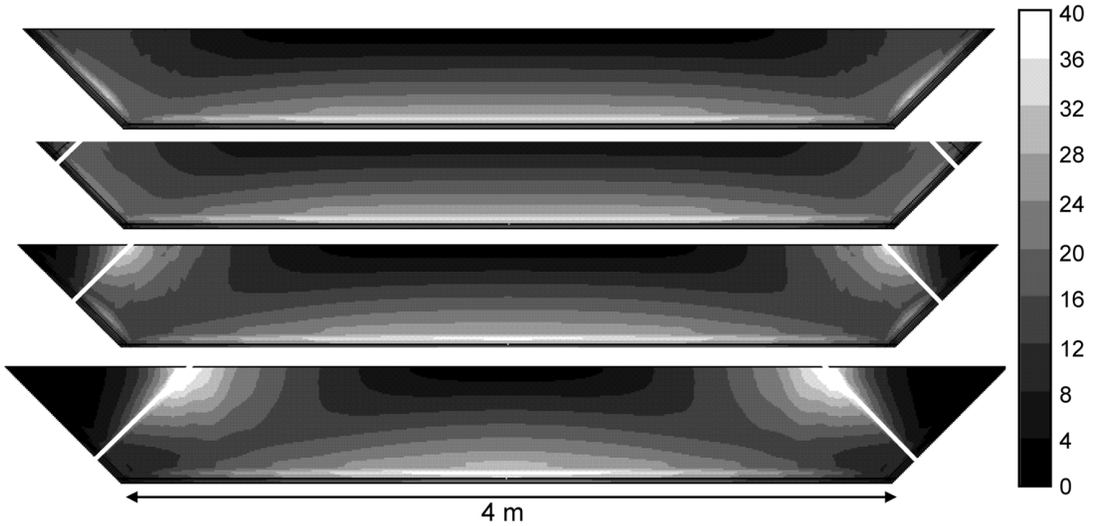

Figure 6. Contours of fluid shear stress (Pa) for four increments of simulated vegetation establishment. The white line indicates the edge of the simulated vegetation. Simulated vegetation density and protrusion increase from top to bottom. A maximum shear stress of 123 Pa occurs in the bottom plot near the water surface at the interface between porous zone and main channel flow.

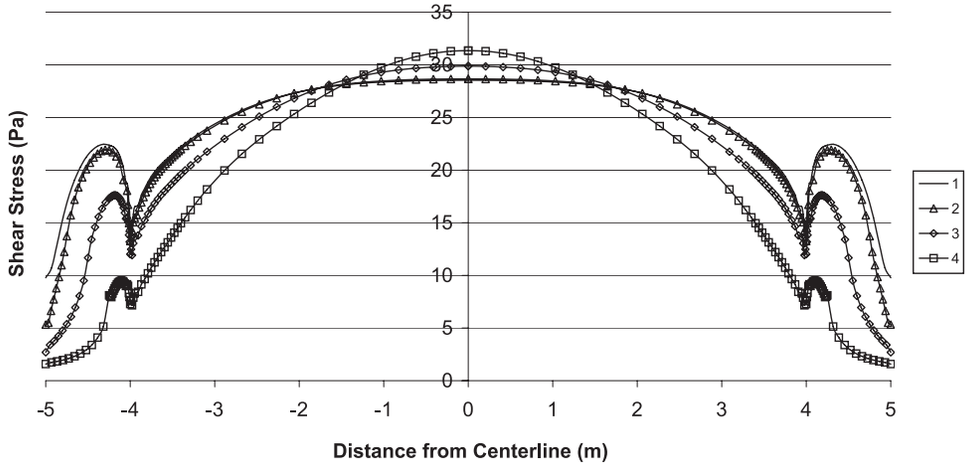

Figure 7. Boundary shear stress profiles for four increments of simulated vegetation establishment.

reduction in boundary shear stress is most significant on the channel banks, as with the velocities. The lowered shear stresses are not limited to flows within the vegetation, but extend beyond the bank toe. This reduction can be attributed in part to the large amount of energy lost in and adjacent to the simulated vegetation zone, which is reflected in the high shear stresses at the vegetation edge near the water surface. In scenario 4, the shear stress at the point of greatest vegetation protrusion is 123 Pa, significantly higher than at any other point in the channel. The magnitude of this high shear stress at the edge of the vegetation may be an artifact of modeling assumptions and limitations to turbulence closure, as this zone typically exhibits highly anisotropic behavior [*Nezu and Onitsuka*, 2001]. However, this zone of shear is consistent with visual observations of vortex shedding in the field, and suggests that this location could be an important source of energy dissipation in vegetated channels. Although the vegetation consumes a large amount of energy and reduces shear stresses in the vicinity of banks, shear stress in the channel center actually increases 9% from scenarios 1 to 4.

A trapezoidal channel was modeled in each of the scenarios presented above. Channels with vertical banks were also modeled in sensitivity tests, yet the resulting velocity profiles varied little from those using a trapezoidal channel with 1:1 slopes when there was thick simulated vegetation on the banks. Similar results were found in simulations involving milder side slopes. Alternatively, with no or minor bank vegetation, there was a more pronounced effect of bank angle on the resulting velocity profiles. With respect to hydraulics, these results suggest that as channels develop thicker bank vegetation, bank morphologic characteristics become less important and are overshadowed by the characteristics of the vegetation on the bank.

4. DISCUSSION

Field data from the United Kingdom and the U.S. Rocky Mountain region indicate a significant scale-dependent effect of bank vegetation that has not been previously accounted for in downstream hydraulic geometry analyses, regime slope models, and shear stress partitioning schemes for gravel bed rivers. The small channels with thick bank vegetation examined in this study have bankfull τ_* and τ values that are roughly twofold those of their thinly vegetated counterparts. The field data and results of the CFD modeling simulations suggest that, as opposed to the traditional focus on relative submergence of vegetation in the vertical dimension, the lateral dimension of channel size relative to the length scale of vegetative roughness is a key missing parameter in understanding shear stress behavior in small streams.

Although there have been numerous physical modeling studies [e.g., *Flintham and Carling*, 1988] examining the effects of channel width-to-depth ratio on shear stress behavior, to our knowledge, no flume study has systematically examined (1) shear stress partitioning using models with banks rougher than the beds and (2) scale-dependent interactions between channel size and vegetation characteristics and their effects on the hydraulic parameters controlling sediment transport and other fluxes in small streams. The CFD simulation results demonstrate the utility and flexibility of using porous media to model various combinations of bed and bank roughness. The CFD modeling approach employed in this study, as well as that of *Kean and Smith* [2004] based on the work of *Houjou et al.* [1990], provide promising computational methods for modeling differentially rough beds and banks that warrant further investigation.

Advances in our knowledge of the scale-dependent influence of bank vegetation have important implications for

restoration design of streams based on "tractive force" (dimensionless shear stress criterion), regime, and analytical approaches [e.g., *Copeland and McComas*, 2001]. For example, *Millar* [2005] presented theoretical regime equations for mobile gravel bed rivers with stable banks that include terms representing relative bank strength as affected by vegetation. However, in selecting a method for shear stress partitioning, Millar was forced to rely on relationships developed in flumes with bed roughness equaling or exceeding bank roughness in all cases [*Knight*, 1981; *Knight et al.*, 1984; *Flintham and Carling*, 1988]. The lack of a shear stress partitioning method that accounts for the scale-dependent effects of bank vegetation introduces uncertainty into estimates of the sediment transport capacity and sediment continuity in small, differentially rough channels designed using these methods.

In analytical approaches to stream restoration, designers often generate a "family" of stable channel designs (Figure 8) that all theoretically convey inflowing water and sediment loads without morphologic change. Uncertainty regarding the coevolution of bank vegetation, hydraulics, and channel form currently confounds design in that shear stress distributions, roughness, and continuity of water and sediment are changing with time (Figure 8). A better understanding of shear stress/vegetation interactions would increase the likelihood of placing channels on a self-organizing trajectory that maintains stability as vegetation reestablishes. This could potentially reduce the reliance on hard structures that "lock in" channels at the desired future width and thereby increase the cost effectiveness of stream restoration in many instances.

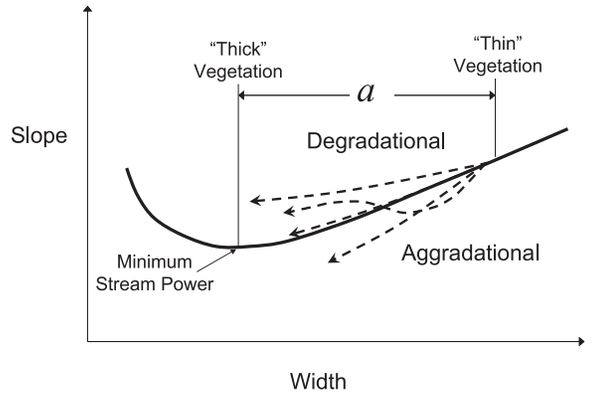

Figure 8. Schematic of theoretical stable channel design solutions for specified inflows of water and sediment with arrows depicting uncertainty in the trajectory and stability of a restoration design as shear stress and conveyance change with vegetation reestablishment along small streams. The range of possible channel widths is also strongly dependent on streamside vegetation as depicted by the range of a, where channel width equals a(bankfull discharge)$^{0.5}$.

Hey [1997] argued that channel slope is not influenced by bank vegetation, and the absence of such an influence can be interpreted as a "problem" for extremal hypotheses such as minimum stream power and maximum sediment transport efficiency. The results of this study indicate that slope is significantly influenced by bank vegetation in channels <20-m wide ($p < 10^{-4}$) and that inferences regarding the realism of extremal hypotheses are spurious in the absence of stream power and shear stress partitioning schemes that account for scale-dependent vegetation effects.

Another aspect of the "problems" associated with extremal hypotheses involves width and slope having different degrees and temporal scales of adjustability [*Hey*, 1997]. The field data used in this study suggest that an increase in slope may be the predominant mode of adjustment in small, thickly vegetated channels, and that differences in depth and grain size account for <20% of the observed twofold increase in bankfull τ_*. If total sediment transport scales roughly with $\tau_*^{1.5}w$, then the fact that widths of the small, thick channels average 60% of their thin counterparts would require τ_* to increase approximately 40% to 45% to maintain an equivalent sediment transport capacity in densely vegetated small channels, all else being equal. The approximately 20% to 25% decrease in bed shear predicted in the CFD simulations for channels of average width in the <20 m wide group (Table 2), when combined with the effect of width reduction would predict a 60% to 70% increase in τ_* to achieve a comparable sediment transport capacity. Thus, the relative influence of bank vegetation on shear stress distributions appears to be potentially greater in natural channels than in the CFD-simulated channels.

Discrepancies in the relative influence of vegetation in natural channels compared with the modeled channels could be explained by a number of factors related to the modeling methods. The channels that were modeled were straight, prismatic channels with no variation in the vegetation characteristics. The existence of topographic complexity, both in the channel characteristics as well as the vegetation characteristics, would seem to influence the results, although the nature of these influences is not clear at present. In the CFD scheme used in this study, modeling the vegetation with varying protrusion characteristics in the downstream direction has minor effects [*Carney*, 2004]. The model was shown to reasonably represent the velocity profiles over and through simulated vegetation in a number of different scenarios; however, in each of the flume experiments used to verify the CFD models and in the simulations described here, the simulated vegetation had regular, homogeneous patterns. Natural vegetation exhibits highly heterogeneous characteristics,

causing expansions, contractions, eddies, and other losses as the flow moves around and through the vegetation. This suggests that future studies should consider the importance of heterogeneous vegetation. While the CFD vegetation representations account for the influence of the vegetation on the momentum equations, they do not account for flow blockage effects caused by vegetation. Particularly in the vicinity of woody vegetation, flow blockage effects would seem to have a dominant effect on the resulting flow fields. Future research could focus on determining appropriate means of accounting for these effects in CFD modeling.

The scale-dependent influence of vegetation on channel hydraulics observed in the CFD simulations appears to support the field observations of *Coon* [1998], who identified an upper limit for the influence of bank vegetation around 20 to 30 m. Similarly, the modeling conducted by *Masterman and Thorne* [1992] suggests at width-to-depth ratios greater than about 15, the effects of riparian vegetation are negligible. In our CFD simulations, the shear stress attributed to the vegetation was 14% and 9% of the total shear stress for 20 and 30 m wide channels, respectively. The *Coon* [1998] channels contained rougher bed material than those used for the case study, so the vegetation probably had less relative influence in these channels than what is suggested by our simulations.

The CFD simulations also point to physical processes that underlie observed differences in channel form in the field studies from the United Kingdom and the western United States, which found that channels with thick, woody bank vegetation were generally narrower and deeper than channels with banks comprised of grasses and thin vegetation. In the simulation of vegetation succession, bank vegetation concentrates flows in the channel center, causing an increase in flow depths for equivalent discharges. Bank vegetation reduces shear stresses in the near-bank zone and increases shear stresses in the channel center. These effects could be more pronounced if erosional and depositional processes were considered. Given time and sufficient supply, aggradation could occur in the low shear stress region along the bank, causing the channel to narrow. In addition, higher shear stresses in the channel center could erode the bed, resulting in deeper channels. These effects would be combined with the increases in bank strength due to the root structure of the vegetation [*Simon and Collison*, 2002], which would provide additional resistance to erosion in narrower channels, especially in smaller channels where rooting depth is on the order of bank height. Thus, vegetation can affect hydraulics in a manner that creates a tendency toward cross-sections that are narrower and deeper than unvegetated channels (but see *Montgomery* [1997] and *Anderson et al.* [2004] for disparate effects due to wood debris and other factors).

Sediment transport capacity in complex channels like those examined in this study is frequently computed using cross-section average shear stress, τ_o [*Julien*, 1995]. In the simulated vegetation succession, however, it was shown that although τ_o increased with successively thicker simulated vegetation due to flow depth increases, the average bed shear stress decreased. Thus, using τ_o to compute sediment transport in these channels may yield inaccurate results without partitioning the shear stress between the bed and vegetation; however, the specific response is complex. The differing shear stress distributions would have nonlinear effects on sediment transport rates depending on the bed characteristics, and the nonuniform distribution of shear stresses could be further magnified in nonprismatic channels [*Lisle et al.*, 2000; *Ferguson*, 2003]. Variations on the CFD modeling approach presented here could be used to provide additional insights into morphologic influences on sediment transport phenomena and assist in the further development and verification of shear stress partitioning schemes.

In summary, these analyses underscore a fundamental gap in our understanding of fluvial processes and hydraulics in wadeable streams with variable bank vegetation. Most previous CFD studies have modeled channels with relatively smooth boundaries for which roughness can be represented using a roughness height and have ignored the impact of bank vegetation. This study demonstrated the need to account for both forms of roughness in CFD modeling of streams less than approximately 30 m wide. Previous research has demonstrated the important influence of vegetation on planform characteristics and meander bend hydraulics [*Thorne and Furbish*, 1995; *Millar*, 2000; *Gran and Paola*, 2001]. CFD modeling focusing on more complex geometries could provide additional insights on the important effects of bank vegetation on planform characteristics of streams. Improved and transferable quantitative tools for predicting shear stress behavior in small streams of different scales and bank conditions could improve the physical basis and effectiveness of stream restoration and simultaneously advance understanding of the inverse problem of stream vulnerability to vegetation disturbance and removal.

5. CONCLUSIONS

The effect of bank vegetation roughness on the hydraulics of natural channels is scale dependent with process shifts evident at widths less than approximately 20 m. This finding has important implications for improvement of shear stress partitioning models used in stable channel design. Because specific mechanisms controlling the apparent scale dependency are difficult to isolate in natural channels, the method of representing vegetation in CFD

applications combined with a porous treatment of rough beds based on the work of *Wiberg and Smith* [1991] and *Carney et al.* [2006] presented in this study can be used to simulate the mechanisms controlling channel form and reveal patterns and scale dependency in hydraulic parameters consistent with field data from channels of different scales and bank vegetation types. Although additional research could improve the parameterization of vegetation in the CFD models, the use of these methods provides a means to better understand the influence of vegetation, on material fluxes, channel evolution, and geomorphic processes in wadeable streams and thereby improve the scientific basis of restoration designs.

Acknowledgments. We are grateful to Ellen Wohl for providing helpful comments on a previous version of this manuscript and to Daniel Gessler who provided both astute suggestions on the CFD modeling and insightful comments on an earlier draft. We also thank two anonymous reviewers for constructive comments that improved the manuscript. This work was supported, in part, by National Science Foundation CAREER Award EAR-0548258.

REFERENCES

Abernethy, B., and I. D. Rutherfurd (2000), The effect of riparian trees on the mass-stability of riverbanks, *Earth Surf. Processes Landforms*, *25*, 921–937.

Andrews, E. D. (1984), Bed-material entrainment and hydraulic geometry of gravel-bed rivers in Colorado, *Geol. Soc. Am. Bull.*, *95,* 371–378.

Anderson, R. J., B. P. Bledsoe, and W. C. Hession (2004), Stream and river width response to vegetation, bank material, and other factors, *J. Am. Water Resour. Assoc.*, *40*, 1159–1172.

Bradbrook, K. F., P. Biron, S. N. Lane, K. S. Richards, and A. G. Roy (1998), Investigation of controls on secondary circulation in a simple confluence geometry using a three-dimensional numerical model, *Hydrol. Processes*, *12*, 1371–1396.

Booker, D. J. (2003), Hydraulic modelling of fish habitat in urban rivers during high flows, *Hydrol. Processes*, *17*, 577–599.

Booker, D. J., D. A. Sear, and A. J. Payne (2001), Modelling three-dimensional flow structures and patterns of boundary shear stress in a natural pool-riffle sequence, *Earth Surf. Processes Landforms*, *26*, 553–576.

Buffington, J. M., and D. R. Montgomery (1999), Effects of hydraulic roughness on surface textures of gravel-bed rivers, *Water Resour. Res.*, *35*(11), 3507–3521.

Carney, S. K. (2004), Computational fluid dynamics investigation of vegetative influences in channels of variable bed roughness, M.S. thesis, Dep. of Civ. Eng., Colo. State Univ., Fort Collins.

Carney, S. K., B. P. Bledsoe, and D. Gessler (2006), Representing the bed roughness of coarse-grained streams in computational fluid dynamics, *Earth Surf. Processes Landforms*, *31*, 736–749.

Charlton, F. G., P. M. Brown, and R. W. Benson (1978), The hydraulic geometry of some gravel rivers in Britain, *Rep. IT 180*, Hydraulics Res. Stn., Wallingford, U. K.

Coleman, N. L. (1967), A theoretical and experimental study of drag and lift forces acting on a sphere resting on a hypothetical streambed, *Proc. Int. Assoc. Hydraul. Res.*, *3*, 185–192.

Coon, W. F. (1998), Estimation of roughness coefficients for natural stream channels with vegetated banks, *U.S. Geol. Surv. Water Supply Pap.*, *2441*, 133 pp.

Copeland, R. R., and D. N. McComas (2001), Hydraulic design of stream restoration projects, *ERDC/CHL TR-01-28*, U.S. Army Corps of Eng., Eng. Res. and Dev. Cent., Coastal and Hydraulics Lab., Vicksburg, Miss.

Crowder, D. W., and P. Diplas (2000), Using two-dimensional hydrodynamic models at scales of ecological importance, *J. Hydrol.*, *230*, 170–191.

Darby, S. E. (1999), Effect of riparian vegetation on flow resistance and flood potential, *J. Hydraul. Eng.*, *125*(5), 443–454.

Darby, S. E., and C. R. Thorne (1996), Predicting stage-discharge curves in channels with bank vegetation, *J. Hydraul. Eng.*, *122*(10), 583–586.

Dunn, C., F. Lopez, and M. Garcia (1996), Mean flow and turbulence structure induced by vegetation: Experiments, *Hydraul. Eng. Ser. 51, UILU-ENG 96-2009*, Dep. of Civ. Eng., Univ. of Illinois at Urbana-Champaign, Urbana.

Ferguson, R. I. (2003), The missing dimension: Effects of lateral variation on 1-D calculations of fluvial bedload transport, *Geomorphology*, *56*, 1–14.

Fischenich, J. C. (1996), Velocity and resistance in densely vegetated floodways, Ph.D. dissertation, Dep. of Civ. Eng., Colo. State Univ., Fort Collins.

Fischenich, J. C. (1997), Hydraulic impacts of riparian vegetation: Summary of the literature, *Tech. Rep. EL-97-9*, 63 pp., U. S. Army Corps of Eng., Waterways Exp. Stn., Vicksburg, Miss.

Fischenich, J. C., and S. Dudley (2000), Determining drag coefficients and area for vegetation, *Tech. Note ERDC TN-EMRRP-SR-08*, U. S. Army Corps of Eng., Eng. Res. and Dev. Cent., Vicksburg, Miss.

Fischer-Antze, T., T. Stoesser, P. Bates, and N. R. B. Olsen (2001), 3D numerical modelling of open-channel flow with submerged vegetation, *J. Hydraul. Res.*, *39*(3), 303–310.

Flintham, T. P., and P. A. Carling (1988), The prediction of mean bed and wall boundary shear in uniform and compositely roughened channels, in *International Conference on River Regime*, edited by W. P. White, pp. 267–287, John Wiley, Chichester, U. K.

Fluent Inc., (2003), *Fluent 6.1 User's Guide*, Fluent Inc., Lebanon, N. H.

Gessler, D., and R. N. Meroney (2002), CFD for predicting shear stress in a curved smooth trapezoidal channel, *Proceedings of Hydrology Days 2002*, Colo. State Univ., Fort Collins.

Gran, K., and C. Paola (2001), Riparian vegetation controls on braided stream dynamics, *Water Resour. Res.*, *37*(12), 3275–3283.

Hardy, R. J., S. N. Lane, R. I. Ferguson, and D. R. Parsons (2003), Assessing the credibility of a series of computational fluid dynamic simulations of open channel flow, *Hydrol. Processes*, *17*, 1539–1560.

Hey, R. D. (1979), Flow resistance in gravel-bed rivers, *J. Hydraul. Div. Am. Soc. Civ. Eng.*, *105*, 365–379.

Hey, R. D. (1997), Stable river morphology, in *Applied Fluvial Geomorphology for River Engineering and Management*, edited by C. R. Thorne, R. D. Hey, and M. D. Newson, pp. 223–236, Wiley, Chichester, U. K.

Hey, R. D., and C. R. Thorne (1986), Stable channels with mobile gravel beds, *J. Hydraul. Eng.*, *112*(6), 671–689.

Houjou, K., Y. Shimizu, and C. Ishii (1990), Calculation of boundary shear stress in open channel flow, *J. Hydrosci. Hydraul. Eng.*, *8*, 21–37.

Julien, P. Y. (1995), *Erosion and Sedimentation*, 280 pp., Cambridge Univ. Press, Cambridge, U. K.

Kean, J. W., and J. D. Smith (2004), Flow and boundary shear stress in channels with woody bank vegetation, in *Riparian Vegetation and Fluvial Geomorphology*, *Water Sci. Appl. Ser.*, vol. 8, edited by S. J. Bennet and A. Simon, pp. 237–252, AGU, Washington, D. C.

Knight, D. W. (1981), Boundary shear in smooth and rough channels, *J. Hydraul. Div. Am. Soc. Civ. Eng.*, *107*(7), 839–851.

Knight, D. W., J. D. Demetrious, and M. E. Hamed (1984), Boundary shear in smooth rectangular channels, *J. Hydraul. Eng.*, *110*(4), 405–422.

Lisle, T. E., J. M. Nelson, J. Pitlick, M. A. Madej, and B. L. Barkett (2000), Variability of bed mobility in natural, gravel-bed channels and adjustments to sediment load at local and reach scales, *Water Resour. Res.*, *36*(12), 3743–3755.

Lopez, F., and M. H. Garcia (1997), Open-channel flow through simulated vegetation: Turbulence modeling and sediment transport, *Wetlands Res. Program Tech. Rep. WRP-CP-10*, 106 pp, U.S. Army Corps of Eng., Waterways Exp. Stn., Vicksburg, Miss.

Ma, L., P. J. Ashworth, J. L. Best, L. Elliott, D. B. Ingham, and L. J. Whitcombe (2002), Computational fluid dynamics and the physical modelling of an upland urban river, *Geomorphology*, *44*, 375–391.

Masterman, R., and C. R. Thorne (1992), Predicting influence of bank vegetation on channel capacity, *J. Hydraul. Eng.*, *118*(7), 1052–1058.

Millar, R. G. (2000), Influence of bank vegetation on alluvial channel patterns, *Water Resour. Res.*, *36*(4), 1109–1118.

Millar, R. G. (2005), Theoretical regime equations for mobile gravel-bed rivers with stable banks, *Geomorphology*, *64*, 207–220.

Montgomery, D. R. (1997), What's best on the banks?, *Nature*, *388*, 328–329.

Morvan, H., G. Pender, N. G. Wright, and D. A. Ervine (2002), Three dimensional hydrodynamics of meandering compound channels, *J. Hydraul. Eng.*, *128*(7), 674–682.

Nezu, I., and K. Onitsuka (2001), Turbulent structures in partly vegetated open-channel flows with LDA and PIV measurements, *J. Hydraul. Res.*, *39*(6), 629–642.

Nicholas, A. P. (2001), Computational fluid dynamics modelling of boundary roughness in gravel-bed rivers: An investigation of the effects of random variability in bed elevation, *Earth Surf. Processes Landforms*, *26*, 345–362.

Nicholas, A. P., and S. J. McLelland (2004), Computational fluid dynamics modelling of three-dimensional processes on natural river floodplains, *J. Hydraul. Res.*, *42*(2), 131–143.

Nicholas, A. P., and G. H. Sambrook-Smith (1999), Numerical simulation of three-dimensional flow hydraulics in a braided channel, *Hydrol. Processes*, *13*, 913–929.

Pasche, E., (1984), Turbulence mechanism in natural streams and the possibility of its mathematical representation (in German), *Mitt. Inst. Wasserbau Wasserwirtsch, Rheinisch Westfael. Tech. Hochsch. Aachen*, *52*.

Prinos, P., D. Sofialidis, and E. Keramaris (2003), Turbulent flow over and within a porous bed, *J. Hydraul. Eng.*, *129*(9), 720–733.

Rahmeyer, W., D. Werth, and R. Cleere (1995), The study of resistance and stability of vegetation in flood channels, *Utah State Univ. Lab Rep. USU-376*, Waterways Exp. Stn., U.S. Army Corps of Eng., Vicksburg, Miss.

Rameshwaran, P., and P. S. Naden (2003), Three-dimensional numerical simulation of compound channel flows, *J. Hydraul. Eng.*, *129*(8), 645–652.

Raupach, M. R., and R. H. Shaw (1982), Averaging procedures for flow within vegetated canopies, *Boundary Layer Meteorol.*, *22*, 79–90.

Shams, M., G. Ahmadi, and D. Smith (2002), Computational modeling of flow and sediment transport and deposition in meandering streams, *Adv. Water Resour.*, *25*, 689–699.

Shimizu, Y., and T. Tsujimoto (1994), Numerical analysis of turbulent open channel flow over a vegetation layer using a k-ε turbulence model, *J. Hydrosci. Hydraul. Eng.*, *11*(2), 57–67.

Simon, A., and A. J. C. Collison (2002), Quantifying the mechanical and hydrologic effects of riparian vegetation on streambank stability, *Earth Surf. Processes Landforms*, *27*, 527–546.

Snedecor, G. W., and W. G. Cochran (1989), *Statistical Methods*, 8th ed., 503 pp., Iowa State Univ. Press, Ames.

Soar, P. J., and C. R. Thorne (2001), Channel restoration design for meandering rivers, *Rep. ERDC/CHL CR-01-1*, U.S. Army Eng. Res. and Dev. Cent., Vicksburg, Miss.

Thorne, S. D., and D. J. Furbish (1995), Influences of coarse bank roughness on flow within a sharply curved bend, *Geomorphology*, *12*(3), 241–257.

Tsujimoto, T., T. Shimizu, and T. Okada (1991), Turbulent structure of flow over rigid vegetation-covered bed in open channels, *KHL Prog. Rep. 1*, Hydraul. Lab., Kanazawa Univ., Kanazawa, Japan.

Wiberg, P. L., and J. D. Smith (1991), Velocity distribution and bed roughness in high gradient streams, *Water Resour. Res.*, *27*(5), 825–838.

Wohl, E. (2000), *Mountain Rivers*, *Water Resour. Monogr. Ser.*, vol. 14, AGU, Washington, D. C.

Wu, W., W. Rodi, and T. Wenka (2000), 3D numerical modeling of flow and sediment transport in open channels, *J. Hydraul. Eng.*, *126*(1), 4–15.

Yakhot, V., and S. A. Orszag (1986), Renormalisation group analysis of turbulence: I. Basic theory, *J. Sci. Comput.*, *1*, 1–51.

Yen, B. C. (2002), Open channel flow resistance, *J. Hydraul. Eng.*, *128*(1), 20–39.

R. J. Anderson, Morrison-Maierle, Inc. 1 Engineering Place, Helena, MT 59602, USA. (randerson@m-m.net)

B. P. Bledsoe, Department of Civil and Environmental Engineering, Colorado State University, D. B. Simons Building at the Engineering Research Center, 1320 Campus Delivery, Fort Collins, CO 80523, USA. (brian.bledsoe@colostate.edu)

S. K. Carney, Riverside Technology, Inc., 2950 E. Harmony Road, Suite 390, Fort Collins, CO 80528, USA. (shaun.carney@riverside.com)